

REAL TIME DETECTOR FOR CYCLOSTATIONARY RFI IN RADIO ASTRONOMY

Rodolphe Weber¹, Christian Faye²

1.LESI-ESPEO, Université d'Orléans BP 6744, 45067 Orléans cédex 2, France

Tel: +33 2 38494562 ; fax: +33 2 38417245 ; e-mail: weber@lesi.univ-orleans.fr

2. ETIS-ENSEA, 6 Avenue du Ponceau, 95014 Cergy-Pontoise, France ; e.mail : faye@ensea.fr

ABSTRACT

The negative impact of radio frequency interferences on the quality of radio astronomical observations is a matter of increasing concern for the radio astronomy community. The integrity of the data can be preserved by detecting the interference in order to blank the receiver in real time. The proposed detector uses cyclostationary properties of the interference. It converts the known hidden periodicity into a periodic signal which can be easily detected. In this paper, the method is explained and simulations applied to typical interferences are presented. Finally, a dedicated hardware implementation using programmable logic array is proposed.

1 INTRODUCTION

As a consequence of the development of telecommunications and radio positioning by satellites, radio astronomers have to deal with an increasing number of unworkable observations polluted by man-made radio interferences [1]. Notably, communication and navigation satellites using widespread modulations are the source of an increasing number of medium and low level out-of-band signal component (see Fig. 1). Although weak compared to the noise at the receiver level, these intermittent and fluctuating signals may pollute entire observation sequences. One solution to this problem is to suspend in *real time* the functioning of the receiver when such an unwanted signal is detected. This technique is known as time-blanking.

Within this technique, several methods of interference detection have been proposed. Most of them are based on real time comparison between the measured spectrum and some adequate spectral standard [2], [3], [4]. These methods, which are often specific and computation requiring, usually rely on characteristics of the expected undisturbed signal. So, it seemed useful to us to propose a more efficient and less computation demanding detection method, which could take advantage of some *a priori* information about the interference. In view of the generalization of radio electric emissions using numerical modulations, we turned our attention to the cyclostationary properties of this class of signals,

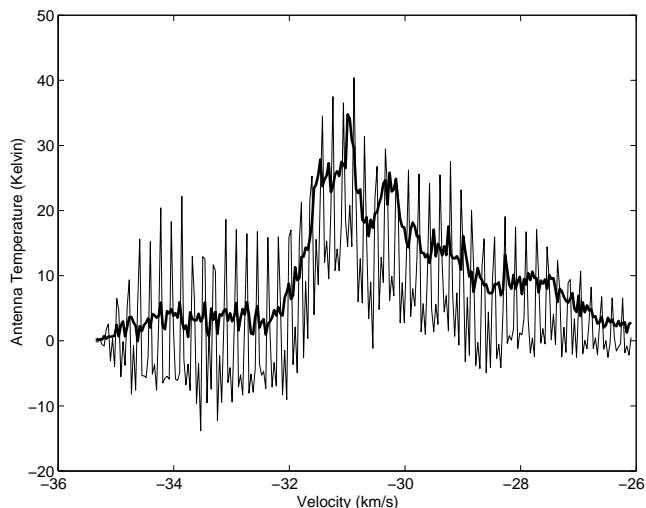


Figure 1: Spectra of the OH radical measured with the Nançay decimetric radio telescope and polluted by spread spectrum RFI. The thick line represents the expected profile and the thin line represents the contaminated one.

and more precisely chose to detect their hidden periodicity.

In the first section, we will explain how the cyclostationary properties of the interference signal are used. The second section will present some simulation results to assess the detector performances on typical interference signals. The last section will develop the hardware implementation of the algorithm on an FPGA¹ component, for real time operation.

2 PRINCIPLE OF THE DETECTOR

An interference signal $b(t)$ is said to be cyclostationary, if its autocorrelation function $R(t, \tau)$ is periodic in t (time). Let us quote T this periodicity, called *hidden periodicity*, because it is not visible on the time representation of the signal. We will assume that this hidden periodicity is known :

¹Field Programmable Gate Array

$$R(t + T, \tau) = R(t, \tau) \quad (1)$$

Usually, the cyclostationary character of a signal emerges from its cyclic spectrum $S(\alpha, \nu)$, the frequency representation of $R(t, \tau)$, where α and ν are respectively the cyclic and the spectral frequencies, dual of t and τ (in that order). As a matter of fact, this 2D representation unveils that the spectral power of the perturbation signal is only located at discrete values of α , which are natural multiples of $1/T$ [5] (see Fig. 2). On the contrary, for the useful signal $u(t)$, which in our case is stationary and Gaussian, the spectral power lies entirely on the axis corresponding to the cyclic frequency $\alpha = 0$. So, the presence of a significant power at the discrete frequencies $\alpha_k = k/T$ ($k \neq 0$) is a discriminating indicator to choose between the two hypothesis :

$$H_0 : s(t) = u(t) \quad (2)$$

$$H_1 : s(t) = u(t) + b(t) \quad (3)$$

Unfortunately, like most 2D methods, this technique is heavy in terms of computation burden and is consequently hard to retain for real time applications. To overcome this major drawback, the proposed detector reduces the 2D problem to a an easy to handle 1D case, while preserving the possible cyclic signature of the interference. The idea, to put it simply, is to project the cyclic spectrum $S(\alpha, \nu)$ upon the α cyclic frequency axis (see Fig. 2). Practically, the projection $P(\alpha)$ of the cyclic spectrum is computed by an autocorrelation conducted on the Fourier transform of the analytical signal, quoted $S_\alpha(\nu)$, associated with the received signal $s(t)$:

$$P(\alpha) = \int_{-\infty}^{+\infty} S_\alpha(\nu) S_\alpha^*(\nu - \alpha) d\nu \quad (4)$$

The use of the analytical signal prevents the appearance of spurious spectral lines that would result from the correlation between positive and negative frequencies for the real signal. The projection $P(\alpha)$ is composed of a discrete line spectrum corresponding to the cyclostationary interference $b(t)$, and a continuous spectrum associated with the useful signal $u(t)$ (see Fig. 2). Using an inverse Fourier transform, the time dual of $P(\alpha)$, noted $m(t)$, contains a T -periodic component, which can be extracted by a simple T -synchronous averaging or $1/T$ -comb filtering. For obvious practical reasons, $m(t)$ is computed directly as the squared modulus of the analytical signal associated with the signal $s(t)$:

$$m(t) = TF^{-1}[P(\alpha)](t) = |s_\alpha(t)|^2 \quad (5)$$

where $s_\alpha(t)$ is the analytical signal associated to $s(t)$ and TF^{-1} represents the inverse Fourier transform.

As can be seen in Fig. 3, the complete algorithm reduces to two linear filtering : a Hilbert filtering to elaborate the analytical version of $s(t)$ and a comb filtering to

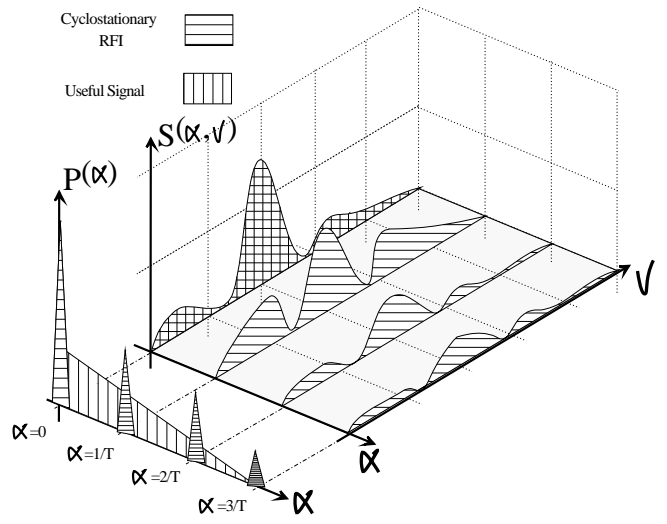


Figure 2: 2D representation, $S(\alpha, \nu)$ of a cyclostationary signal (with a hidden periodicity T) mixed with a stationary one. $P(\alpha)$ is the "projection" of $S(\alpha, \nu)$ upon the α cyclic frequency.

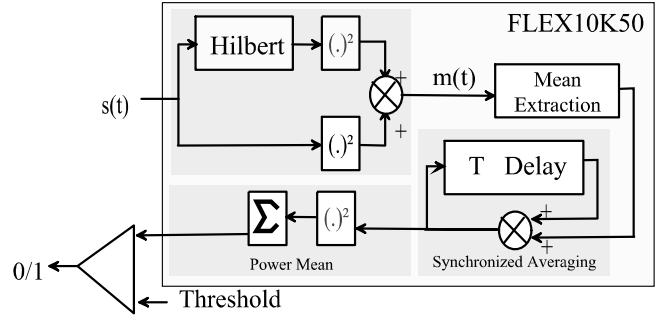


Figure 3: Principle of the algorithm. $m(t)$ is the square modulus of the analytical signal associated with $s(t)$. The synchronized averaging realizes a comb filtering of $m(t)$. The Fourier transform of $m(t)$ is $P(\alpha)$ (see Fig. 2).

extract the T -periodic component from $m(t)$, plus a few elementary adding and squaring operations, all easily implementable in real time.

3 SIMULATIONS

The method described above has been tested numerically on synthetic signals reproducing real world situations encountered at Nançay Decimetric Radio telescope (NRT). Among the interferences frequently disturbing radio astronomers are the widespread spectrum signals emitted by the radio positioning satellites (GLONASS² or GPS³). These signals possess an hidden periodicity, either due to the very structure of their modulation (*e.g.* the pulse rate for BPSK⁴ modulations or a frame synchronization coding), or due to a frequency shift which

²GLOBAL Navigation Satellite System

³Gobal positioning System

⁴Binary Phase Shift Keying

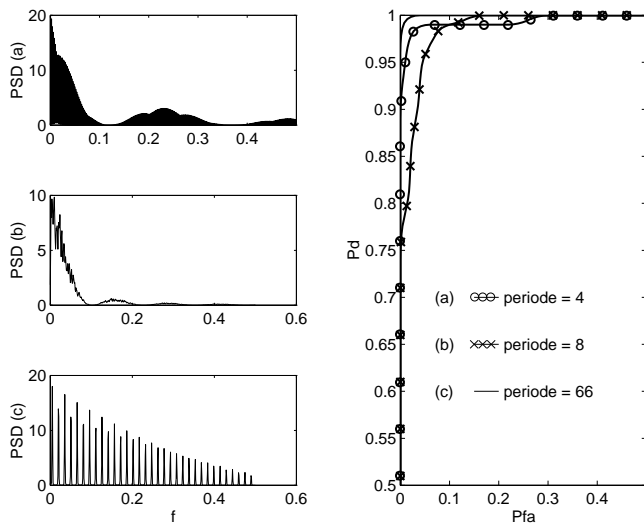


Figure 4: P_{fa} against P_d for three types of cyclostationary RFI : in (a) and (b) the hidden periodicity is linked with the width of a BPSK elementary pulse, in (c) the hidden periodicity is linked with the binary key of a BPSK modulation. The RFI to noise ratio is -14 dB. $1024 * T$ samples are used for each one of the 100 trials.

destroys a periodicity initially found in the signal (*e.g.* a Doppler shift affecting the binary key used to code the information). The figures 4.a, 4.b and 4.c show typical spectra of three interferences $b(t)$ used in the simulations. Their hidden periodicity, T , expressed in normalized time, are respectively equal to 4, 8 and 66. The useful signal is a centered white Gaussian noise. The detection of the period T is carried out by a synchronized averaging over $1024 * T$ samples and a computation of the mean power over the period.

Figure 4 represents the Receiver Operating Characteristics curves plotted for 100 trials of the H_0 and H_1 hypothesis. The results show that interferences having an interference to signal ratio (ISR) of -14 dB are detected with a 95 % detection and a 5 % false alarm probability. As a comparison, with the same number of samples as in the one used in figure 4.c, the detection method currently in use at NRT (apply a threshold to power spectral density) would only reach a -1 dB ISR, with the most favorable spectral resolution. Besides, the asymptotic behavior shows that allowing the multiplication of the detection time by a factor 100, leads to a 10 dB lowering of the detection threshold.

4 IMPLEMENTATION

The proposed detector has been implemented on an electronic circuit, and is currently under test with the aim of conducting experiments on actual signals at NRT. Here are the details of the realization (see Fig. 5 and Fig. 6):

At first, the signal is conditioned prior to its numerical processing. In addition to the anti aliasing filter, an

automatic gain control (AGC) has been added. It allows to get rid of the fluctuations (≈ 10 %) usually affecting the useful signal. After a conversion from analog to digital form, the 12 bit digitized signal is applied to the detection algorithm above described (see Fig. 3). The sampling rate is currently $3 \cdot 10^6$ samples/sec.

The implementation was conducted on a single FPGA⁵ circuit FLEX 10K50 from Altera. This component contains a large number of logic gates ($\approx 50,000$) as well as a random access memory (RAM) which can be used as a mean to store data. The Hilbert filtering is performed in fixed point calculation under the form of a 33 coefficients transversal filter. The included RAM enables the memorization of the partial products in a Look Up Table, which leads to the complete parallel processing of multiplication operations. In terms of computation velocity, the advantage is considerable. The rate of $100 \cdot 10^6$ samples/sec can be reached. The other functions (squaring, centering, synchronous averaging, integration) have been performed in floating point calculation (8 bit for mantissa and 7 bit for exponent) to avoid any under or overflow problem. The realization of the T -delay line used in the synchronized averaging also takes advantage of the on-chip RAM to ease the control of a FIFO⁶ stack. The development tools supplied with the FLEX 10K50 reduces the task of programming the component. On the other hand, the large number of pins on the circuit (403 in all) makes the routing task very tedious by conventional means.

5 CONCLUSION

In the scope of time blanking techniques, the proposed detector leads to an original real time exploitation of the cyclostationary properties of unwanted signals. The present description is limited to signals of known hidden periodicity. However it could be improved to deal with unknown periodicity. Simulations have shown that it can efficiently suppress interferences of high ISR, — compared to what is usually considered as a disturbing level in radio astronomy, *i.e.* -50 dB—. Besides, the use of an FPGA component leads to a compact and speedy real time hardware realization, where the complete algorithm was successfully implemented. The proposed method may also be used in other application fields, such as the monitoring of sets of gear-wheels in turbines, or the fast survey of the radio electrical environment in telecommunications.

Acknowledgment : The authors are grateful to the Nançay Scientific Unit of the Paris Observatory, USR No. B704 of the French CNRS for its financial support.

References

- [1] McNally D. "The vanishing universe - adverse environmental impacts on astronomy", *Cambridge Uni-*

⁵Field Programmable Gate Array

⁶First In, First Out

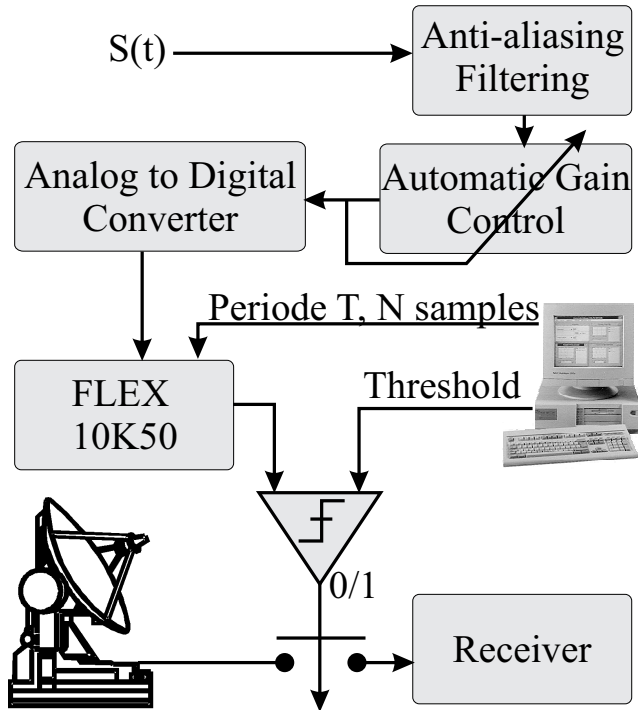
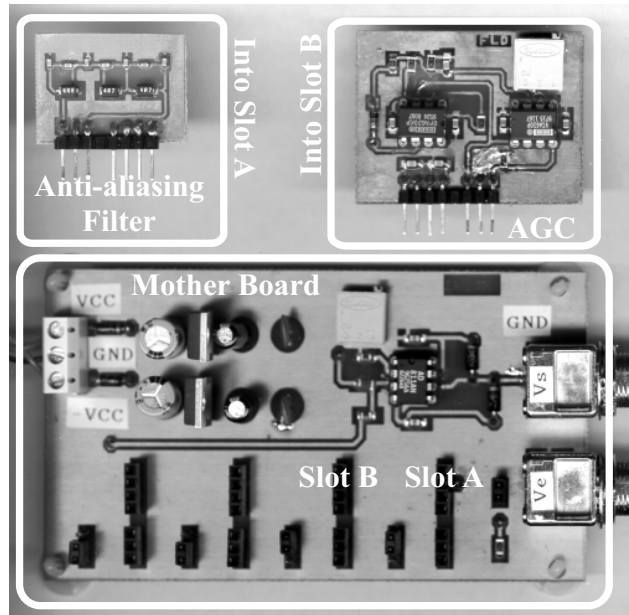


Figure 5: Principle of the detector. The contents of the FLEX 10K50 is detailed in Fig.3. The input of the FLEX 10K50 are the hidden periodicity T and the number N of period which will be averaged.

iversity Press, Part III, pp.71-113, 1994.

- [2] Weber R., Faye C., Biraud F. and Dansou J., "Spectral Detector for interference time blanking using quantized correlator" *Astronomy & Astrophysics Supplement Series*, 126, pp.161-167, november 1997.
- [3] Weber R., Faye C. "Coarsely quantized spectral Estimation of Radio astronomic Sources in Highly Corruptive Environments", to be published in chap. 8 of "Signal analysis and Prediction" editors Prochazka et al., Birkhäuser, Boston, 1998.
- [4] Lacasse R. "RFI excision on the spectral processor and why it is not used", *Proc. of Workshop on New Generation of Digital Correlators*, National Radio Astronomy Observatory, USA, 1993.
- [5] Gardner W.A. et Spooner C.M., "Signal interception: Performance advantages of cyclic-feature detectors" *IEEE Transactions on communications*, Vol.10, no. 1, pp149-159, 1992.

a) Analog Board



b) Digital Board

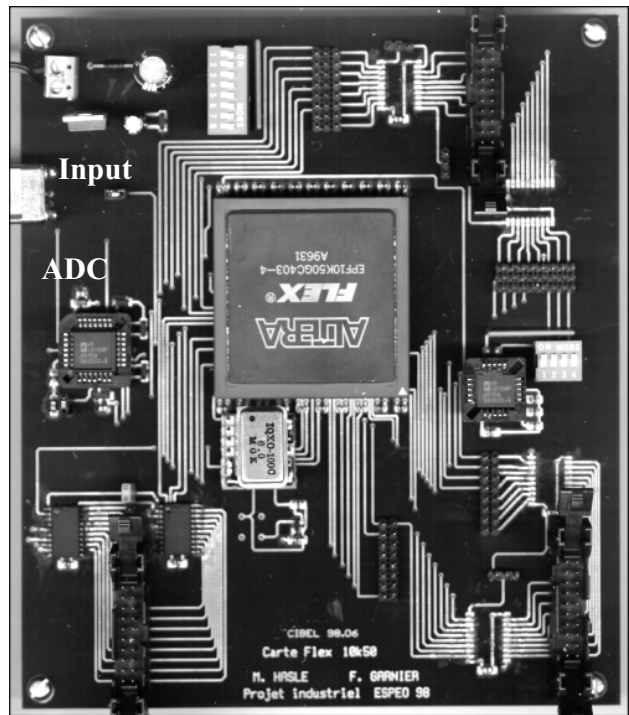


Figure 6: Hardware implementation of the detector. **(a) Analog board:** The anti-aliasing filter is a 7th Cauer low-pass filter. Its cut-off frequency is 1.5 MHz. The automatic gain control uses a wideband voltage controlled amplifier VCA 610 linked with a wideband operational amplifier OPA 620. These two boards are plugged into a mother board. **(b) Digital board:** 4 layers board with a FLEX 10K50, an Analog to Digital Converter, a 6 MHz clock and an EEPROM for FLEX configuration.